Solid State Ionics 1 (1980) 211–221

SOLID ELECTROLYTE PROPERTIES OF LaF_3

J. SCHOONMAN, G. OVERSLUIZEN* and K.E.D. WAPENAAR
Solid State Department, Physics Laboratory, State University, 3508 TA Utrecht, The Netherlands

Received 26 March 1980

The small-signal ac response of cells with LaF_3 or the solid solutions $La_{1-x}Ba_xF_{3-x}$ and ionically blocking electrodes has been measured in the frequency range $0.1-3 \times 10^4$ Hz, and for temperatures from 220 to 650 K. The bulk electrolyte conductivity of LaF_3 crystals is anisotropic up to 415 K. For polycrystalline samples grain boundary effects markedly influence the frequency dispersion. Above room temperature these effects mask the bulk electrolyte conductivity in the accessible frequency range. The composition dependence of the bulk electrolyte conductivity of $La_{1-x}Ba_xF_{3-x}$ solid solutions is compared with ^{19}F NMR data, and used to discuss recently reported association effects in LaF_3. Reported anomalies in the electrical properties of LaF_3 are used to exemplify the need to study the frequency dispersion over a wide frequency range.

1. Introduction

Fluoride ion conduction in LaF_3 (tysonite structure) has been studied extensively. The electrical properties and the magnetic resonance line narrowing have been reviewed recently [1]. The current literature [1] clearly reveals a lack of consistency in the ionic transport parameters of crystals and powders of LaF_3. Its reactivity towards oxygen and water vapor appears to interfere strongly in the experimental characterization of the ionic transport. Due to the formation of oxygen-rich surface layers frequency-dependent effects have been observed. Such layers even tend to mask the intrinsic conductivity region [2]. Crystals with geometric factors greater than four exhibit, however, monofrequency conductivities which lead to Arrhenius plots in the range 300–800 K, in which usual association, extrinsic and intrinsic regions can be discerned [2]. For temperatures greater than 800 K a negative deviation from Arrhenius behavior occurs. This behavior resembles the Faraday transition commonly observed in the high-temperature conductivity of fluorites. While this transition is an intrinsic property of fluorites [3], in LaF_3 it is related to

* Present address: Laboratory of Physical Chemistry, University of Technology, Eindhoven, The Netherlands.

the oxygen-rich surface layers, which have been modeled as a temperature-independent resistance of about 10^2 to 10^3 Ω in series with the sample [2].

Nagel and O'Keeffe [4] reported the conductance of LaF_3 crystals to become frequency dependent in the range ≈475–775 K, possibly due to electrode polarization effects. Similar effects were observed for sintered pellets of anion-deficient tysonite-related solid solutions like $La_{0.95}Sr_{0.05}F_{2.95}$.

To date ac impedance measurements have been performed only at a few fixed frequencies, this being the main cause of the ambiguities in the bulk electrolyte conductivities. The present paper reports the small-signal ac response of cells with single crystalline as well as polycrystalline LaF_3, and $La_{1-x}Ba_xF_{3-x}$ solid solutions provided with ionically blocking electrodes over a wide range of frequencies and temperatures. True bulk electrolyte conductivities are evaluated from the frequency dispersion. In addition, the role of grain boundaries is emphasized. The composition dependence of the conductivity of the solid solutions is shown to be concordant with reported ^{19}F magnetic resonance line narrowing data. The consequences for association of defects in LaF_3 are discussed.

2. Experimental aspects

Melt-grown single crystals of LaF_3, and polycrystalline ingots of the anion-deficient solid solutions $La_{1-x}Ba_xF_{3-x}$ ($0.005 \leqslant x \leqslant 0.10$) were obtained from Dr. H.W. den Hartog, Solid State Physics Laboratory, State University of Groningen. CdF_2 has been employed as a scavenger in the melt-growth procedure. X-ray diffraction studies confirmed the solid solution to be single-phase, and to have the tysonite structure.

In order to study the role of grain boundaries in addition to the bulk ionic conductivities part of the materials were ground in a mechanical grinder for $\frac{1}{2}$ h, and pellets were obtained by mechanical pressing: 5.4×10^7 kg/m^2. Densities varied from 80 to 90%. Discs of the anion-excess solid solutions were cut from the polycrystalline ingots. These samples have considerably less grain boundaries than the pressed pellets. The electrode contact surfaces of the discs, and of the LaF_3 crystals were polished. Electrode contact surfaces varied typically from 1.8×10^{-5} to 6.4×10^{-5} m^2, while thicknesses were from 1×10^{-3} to 6×10^{-3} m. As electrode contact material a platinum paint (Leitplatin 308A, Degussa) was employed. The admittance parameters were recorded for temperatures from 220 to 650 K in the frequency range 0.1 Hz–30 kHz, using impedance bridges and a frequency response analyser, which have been described before [5]. As ambient dry, oxygen-free nitrogen was used.

3. Results

Fig. 1 presents examples of admittance plots in the complex-plane representation

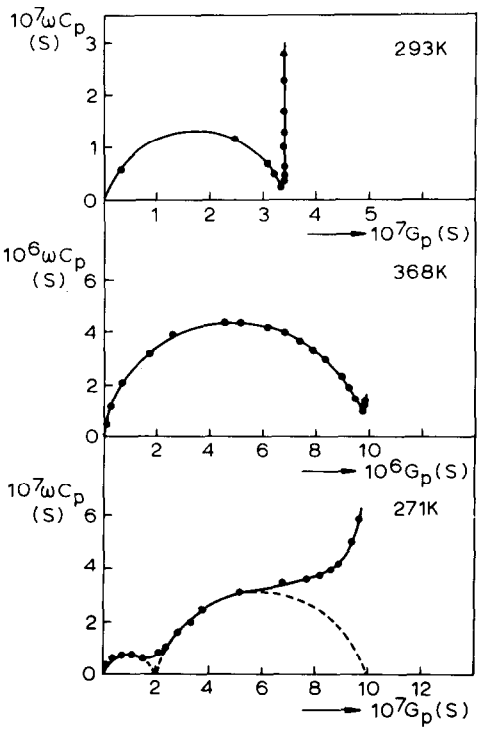

Fig. 1. Complex admittance plots ($Y = G_p + i\omega C_p$) for undoped LaF_3 crystals at 293 and 368 K, and for polycrystalline $La_{1-x}Ba_xF_{3-x}$ ($x = 5 \times 10^{-3}$) at 271 K. Frequency range 0.1 Hz–30 kHz.

for cells with LaF_3 crystals at 293 and 368 K, and with a polycrystalline disc of $La_{1-x}Ba_xF_{3-x}$ ($x = 5 \times 10^{-3}$) at 271 K. Varying the sample dimensions showed the high-frequency intercepts with the real axis to represent true bulk conductances.

For LaF_3 crystals the bulk electrolyte conductivity was measured parallel and perpendicular to the crystallographic c axis. These data are presented in fig. 2, along with data reported by Sher et al. [6]. The results reported by Chadwick et al. [2] for a high-purity LaF_3 crystal at 50 kHz with a geometric factor greater than four, and the present data are in general concordance as to the magnitude of the conductivity.

For the polycrystalline solid solutions $La_{1-x}Ba_xF_{3-x}$ the bulk electrolyte conductivities are given in fig. 3. It is worth noting that for temperatures only below room temperature in the accessible frequency range the date can be modeled accurately with two, slightly depressed, semicircular arcs, required to determine bulk conductance data (cf. fig. 1, $T = 271$ K). Fig. 4 presents the isothermal conductivities of the solid solutions against the solute content for $T = 250$ K. The conductivity activation enthalpies are gathered in table 1, together with literature data.

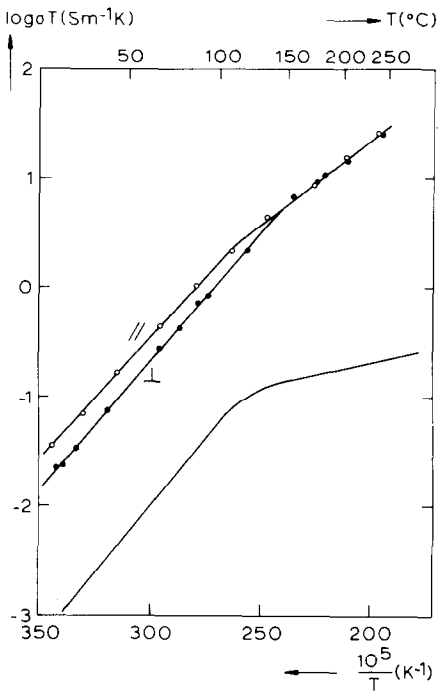

Fig. 2. The bulk electrolyte conductivity of a LaF_3 single crystal measured parallel (○) and perpendicular (●) to the c axis. The full line represents the data reported by Sher et al. [6].

In the range 300–650 K the admittance plots for cells with pressed pellets or polycrystalline discs of $La_{1-x}Ba_xF_{3-x}$, and for cells with pressed pellets of LaF_3 closely resembled the data presented for a LaF_3 crystal at 368 K (cf. fig. 1). The intercepts with the real axis are plotted as log σT versus T^{-1} in fig. 5 along with the true electrolyte conductivities. Huge discrepancies exist between thus determined conductivities of pressed, polycrystalline, and single crystalline materials.

4. Discussion

The admittance plots for LaF_3 crystals show that the high-frequency data require an equivalent circuit composed of a frequency-independent (bulk) capacitance, $C_{\sim}$, in parallel with a frequency-independent (bulk) resistance, R_B. At low frequencies the depressed arcs indicate a series combination of R_B and a frequency-dependent interface impedance. Frequency-dependent interface impedances are found widespread, and have received attention in the recent literature [8,9]. A systematic investigation into the mechanistic origin of such impedances (constant-phase

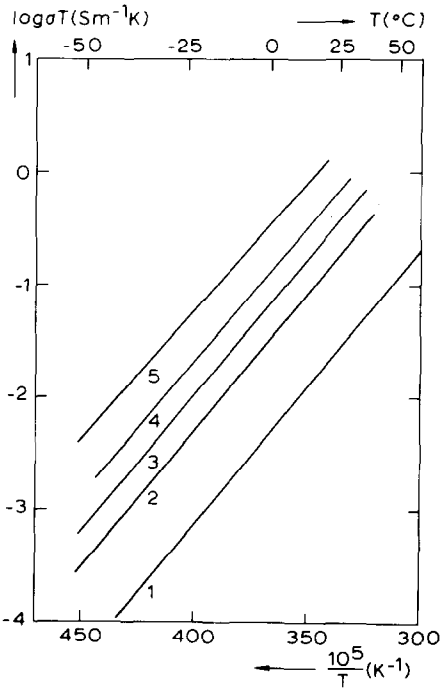

Fig. 3. Bulk electrolyte conductivity of LaF_3 and the solid solutions $La_{1-x}Ba_xF_{3-x}$. (1) Undoped LaF_3 ($\sigma_\perp$ from fig. 2), (2) $x = 5 \times 10^{-3}$, (3) $x = 1 \times 10^{-2}$, (4) $x = 10^{-1}$ and (5) $x = 5 \times 10^{-2}$.

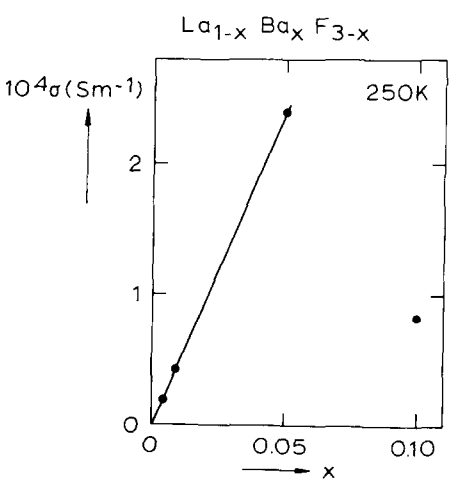

Fig. 4. Conductivity isotherm for $La_{1-x}Ba_xF_{3-x}$ at 250 K.

Table 1

Activation enthalpies for conduction and diffusion in LaF_3 crystals, and the polycrystalline anion-deficient solid solutions $La_{1-x}Ba_xF_{3-x}$

Material	Temperature range (K)	Method	ΔH (eV)	Ref.
LaF_3	300–400	σ	0.38 ± 0.05	[2]
	400–555	σ	0.28 ± 0.05	[2]
	555–800	σ	0.80 ± 0.05	[2]
LaF_3	300–430	σ	0.46	[6]
	430–830	σ	0.084	[6]
LaF_3 ($\perp$, $\parallel c$ axis)	300–450	^{19}F NMR	0.43 ± 0.05	[7]
LaF_3	290–400	σ	0.46 ± 0.01	this work
($\perp c$ axis)	400–525	σ	0.27 ± 0.01	this work
LaF_3	290–400	σ	0.44 ± 0.01	this work
($\parallel c$ axis)	400–525	σ	0.27 ± 0.01	this work
$La_{1-x}Ba_xF_{3-x}$ ($5 \times 10^{-3} \leq x \leq 1 \times 10^{-1}$)	220–315	σ	0.48 ± 0.02	this work

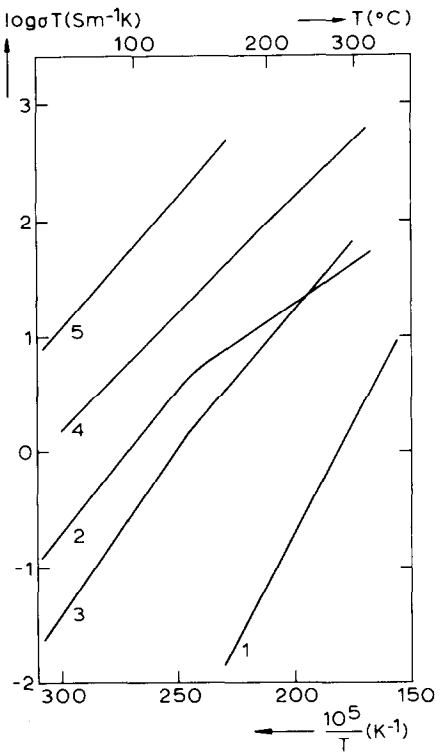

Fig. 5. The electrical conductivity of undoped LaF_3 and the solid solutions $La_{1-x}Ba_xF_{3-x}$ for temperatures above room temperature. (1) LaF_3, pressed pellet, (2) LaF_3, single crystal (data from fig. 2), (3) $La_{0.95}Ba_{0.05}F_{2.95}$, pressed pellet, (4) same, polycrystalline disc, (5) same, extrapolated bulk electrolyte conductivity (cf. fig. 3).

angle impedances) has not yet appeared, except for pure Warburg response which leads to a $\omega^{-1/2}$ dependence of the real and imaginary parts. Armstrong and co-workers [10,11], however, have shown convincingly that surface roughness at the electrode–electrolyte interface leads to Warburg-like effects and consequently to depression of the arcs. Here, we will focus attention on the resistive elements in the equivalent circuit.

The frequency dispersion obtained with the polycrystalline discs of $La_{1-x}Ba_xF_{3-x}$ (cf fig. 1) can be modeled using a grain boundary polarization model [12], i.e. blocking of mobile charge carriers at grain boundaries in the interior of the sample. Ideally, this can be accounted for by a parallel RC combination, representing the grain boundary effect, in series with the bulk electrolyte resistance, R_B, and an interfacial capacitance, if ionically blocking electrodes are employed. As the response of this electrolyte also reveals depressed arcs the capacitances are in fact to be replaced by frequency-dependent impedances. If R_{gb} stands for the grain boundary resistance the intercept of the first arc with the real axis represents $(R_{gb} + R_B)^{-1}$, while the second arc intercepts at R_B^{-1} [12], as used in the previous section to obtain the bulk electrolyte conductivities. The data in fig. 5 then indicate that above room temperature the ac response of pressed pellets and polycrystalline discs is governed entirely by the grain boundary polarization effect. The intercepts that can be obtained from the admittance plots represent $(R_{gb} + R_B)^{-1}$. For these materials the second arc goes unnoticed in the accessible frequency range. The specific conductivities plotted in fig. 5 were calculated from conductance data, and the geometric factor, d/O, where d is the sample thickness and O the sample area as usual. In order to specify grain boundary conductivities a different geometric factor is required, i.e. $(AR_{gb})^{-1} \rightarrow \sigma_{gb}$, where the geometric factor A (m^2) is to be related to the grain surfaces. Except for curves 2 and 5 the curves in fig. 5 are given by $\sigma = [\sigma_B^{-1} + (O/d)(A\sigma_{gb})^{-1}]^{-1}$, which reduces for pressed pellets ($R_{gb} \gg R_B$) to $\sigma = (d/O)(A\sigma_{gb})$ (curves 1 and 3). For curves 2 and 5 $\sigma = \sigma_B$. For the polycrystalline disc of $La_{0.95}Ba_{0.05}F_{2.95}$ the data in fig. 1 reveal for $R_B + R_{gb}$ the value 4.07×10^6 Ω, and for R_B the value 9.26×10^5 Ω at 271 K, i.e. R_B and R_{gb} are of the same order of magnitude. For polycrystalline samples A will be smaller than for the pressed pellets. Despite these more favourable circumstances it is still required to measure the polycrystalline samples in the accessible frequency range below room temperature for a reliable determination of R_B. Curves 1 and 3 can be used to calculate activation enthalpies for grain boundary conduction in LaF_3, and in $La_{0.95}Ba_{0.05}F_{2.95}$. The activation enthalpies are 0.91 eV, and 0.55 ($T < 400$ K), and 0.46 eV ($T > 400$ K), respectively, whereby it must be noted that A may be temperature dependent.

Fig. 2 reveals the bulk electrolyte conductivity of LaF_3 to be slightly anisotropic with $\sigma(\parallel c$ axis$) > \sigma(\perp c$ axis), for temperatures up to about 415 K. At room temperature the anisotropy factor is close to 2. This factor slightly decreases upon increasing temperature. In the tysonite structure two types of fluoride ion site need to be considered in a ratio 2:1 [7]. As fluoride ion vacancies, $V_F^{\bullet}$, are believed to

constitute the mobile species, and ^{19}F NMR experiments reveal motional narrowing of the resonant species to occur between 300 and ≈450 K [6,7], anisotropic fluoride ion conductivities via vacancies are to be expected. The present data show that for temperatures greater than 415 K, fluoride ions can interchange easily between the different types of site. The ^{19}F NMR data show that for $T > 500$ all the fluoride ions are in rapid motion [13]. Chadwick et al. [2] report the conductivity of LaF_3 to be anisotropic ($\sigma_\parallel > \sigma_\perp$) in the range 300–870 K. These conductivities cross the intrinsic line. Moreover, for both $\sigma_\parallel$ and $\sigma_\perp$ the slope in the log σT versus T^{-1} plot continuously decreases in this temperature range. These effects have been ascribed to an oxygen-rich layer which can be represented by a temperature-independent resistance of about 10^2 to 10^3 Ω in series with the sample. This model needs some consideration. If the LaF_3 crystal is covered with a layer of resistance R_L then two situations can be discerned, i.e. $R_L > R_B$ and $R_L < R_B$. In the former case, the equivalent circuit used here to describe the grain boundary polarization effect can be employed also, the parallel RC combination now standing for R_L and the capacitance C_L of the layers situated in between the electrolyte, and the blocking electrodes. Under this condition the layer at the sample sides goes unnoticed. In the latter case the layers at the interfaces electrode–electrolyte can go unnoticed, while an enhanced surface conductivity will occur. Under both conditions two semicircular arcs will show up in the admittance plot. In the former case the intercept of the second arc with the real axis represents the true bulk electrolyte conductance G_B, while in the latter case the first intercept represents G_B, and the second intercept the sum of the bulk and of the surface conductance. For fluorites the situation $R_L > R_B$ has been worked out in detail [14], and stresses the necessity to study the dispersion over a wide frequency range in the case of surface degradation effects. That the conductivities are found to cross the intrinsic line [2] is not compatible with an oxygen-rich layer, in which fluoride ion vacancies, $V_F^{\cdot}$, electrically compensate for substitutional oxygens, O_F', since this would represents an $R_L < R_B$ situation, and hence a contribution by surface conduction in addition to bulk conduction. Hydrolysis or reaction with oxygen leads to the formation of LaOF. Its conductivity is about 10^{-1} S m^{-1} at 673 K with an activation enthalpy of 0.39 eV [15]. Hence, a $R_L > R_B$ situation will occur. Monofrequency apparent conductivities could then be smaller than frequency-independent bulk electrolyte conductivities. In all instances R_L will vary with temperature.

Up to about 375 K the present data, and the data reported by Sher et al. [6] exhibit comparable activation enthalpies (cf. fig. 2, table 1). The difference in magnitude of the conductivities in this temperature range may be due to a different oxygen content, or to the presence of the scavenger CdF_2 employed in the growth of the crystals here. Both types of impurity increase the fluoride ion vacancy content. The conductivity of a high-purity crystal [2] is comparable to the present data given in fig. 2. The activation enthalpies for the crystal are 0.38 and 0.28 eV, and have been used to evaluate an impurity–vacancy association enthalpy, i.e. 0.20 eV [2], the impurity being oxygen, or a divalent cation. The changeover from the associa-

tion region to the free-defect region occurs at temperatures where the present data, and the data reported by Sher et al. [6] reveal a decrease in activation enthalpy. The question then arises as to whether association of defects needs to be considered in interpreting the data in fig. 2. The data in fig. 3 reveal activation enthalpies of about 0.48 eV for the solid solutions $La_{1-x}Ba_xF_{3-x}$. The composition dependence in fig. 4 reveals up to the value 0.05 for x a linear conductivity isotherm. For dilute solid solutions it is common practice to calculate mobilities from such isotherms. One can calculate a mobility from the isotherm in fig. 4, and with the Einstein relation the value 3.7×10^{-17} m^2/s is obtained for the diffusion coefficient $D(V_F^{\bullet})$ at 250 K. Lee and Sher [7] report D(NMR) for the range 300–450 K. From their data D(NMR) is calculated to be 9.2×10^{-17} m^2/s at 250 K, and this value is reasonably close to $D(V_F^{\bullet})$. This strongly suggests that association between barium ions, Ba'_{La}, and $V_F^{\bullet}$, if present at all, is of minor importance in the solid solutions $La_{1-x}Ba_xF_{3-x}$. Consequently, activation enthalpies of about 0.48 eV are to be related with free vacancy conduction, and this situation holds for both the solid solutions, and the crystals. The composition dependence of the conductivity of the solid solutions can be used to determine the impurity content of the present undoped crystals. A substantial amount of 675 ppm is obtained.

It has been shown [16] that in the series of anion-deficient tysonite-related solid solutions $La_{0.95}Sr_{0.05}F_{2.95}$, $BiO_{0.1}F_{2.8}$, $Y_{0.73}Ca_{0.27}F_{2.73}$ association becomes increasingly important. The bulk electrolyte conductivities are found to decrease substantially in this sequence. Therefore, optimum solid electrolyte properties for these tysonite-related materials are to be expected for relatively low fluoride ion vacancy contents. In fact, Takahashi et al. [17] observed a maximum in the composition dependence of the solid solutions $Ce_{1-x}Ca_xF_{3-x}$ for $x = 0.05$. A similar tendency is observed for the data presented in fig. 4. Therefore, $La_{0.95}Sr_{0.05}F_{2.95}$, $Ce_{0.95}Ca_{0.05}F_{2.95}$, and the present solid solution $La_{0.95}Ba_{0.05}F_{2.95}$ are close to the composition for which optimum conductivities are expected. An association model, however, is inadequate to explain a maximum in the conductivity isotherm. Instead, ordering of oppositely charged defects can account for this type of composition dependence of the conductivity [18]. These matters are currently under study in our laboratory. Fig. 6 shows how the bulk electrolyte conductivities compare with well-known fluorite-structured solid solutions based upon β-PbF_2 [19,20].

For $T > 375$ K Sher et al. [6] obtain a very small activation enthalpy. The measurements were made on a thin crystalline wafer ($d = 5 \times 10^{-5}$ m) by applying a step voltage, which is equivalent to a monofrequency measurement. Tiller et al. [21] obtained such small activation enthalpies for polycrystalline evaporated LaF_3 films in the range 320–400 K by measuring dc currents as a function of temperature with a constant applied potential. For $T < 320$ K the activation enthalpy is 0.40 ± 0.05 eV which is also smaller than expected. They discuss the anomaly for $T > 320$ K in terms of trapping of the rapidly moving fluoride ions in vacancies in that part of the anion sublattice with which rapid exchange can occur only above 500 K. If interfacial space-charge polarization limits the current due to bulk conductivity this tech-

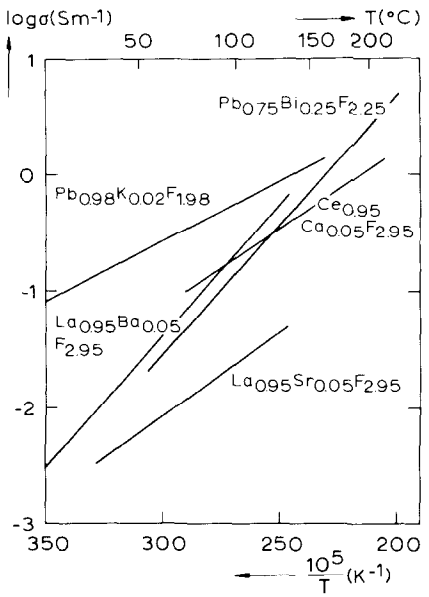

Fig. 6. Bulk electrolyte conductivity of several fluorite (β-PbF_2), and tysonite (CeF_3, LaF_3) structured solid solutions.

nique can yield accurate activation enthalpies [22]. However, the present frequency dispersion of polycrystalline materials clearly reveals that grain boundary polarization will limit the current due to bulk conductivity, as well. In order to clarify the mechanism leading to a decrease in activation enthalpy, studies on dilute solid solutions are currently undertaken.

5. Conclusions

The frequency dispersion in the small-signal ac response of single crystalline and polycrystalline LaF_3 and of polycrystalline $La_{1-x}Ba_xF_{3-x}$ solid solutions provided with ionically blocking electrodes can be used to evaluate reliable bulk electrolyte conductivities, and can give insight into bulk grain boundary effects. These effects strongly limit the current due to bulk conductivity in these solid electrolytes.

The composition dependence of the bulk electrolyte conductivity of $La_{1-x}Ba_xF_{3-x}$ is linear up to $x = 0.05$. Neither association effects, nor defect ordering effects seem to play a role in this concentration regime. The present results indicate that defect–defect interactions reported for nominally pure LaF_3 are unlikely.

Acknowledgement

The authors are grateful to Dr. H.W. den Hartog, Solid State Physics Laboratory, State University of Groningen, The Netherlands, for providing the materials used in this study, and thank Professor Dr. G. Blasse for critically reading the manuscript.

References

[1] Gmelin Handbuch der Anorganischen Chemie, Seltenerdelemente, Teil C3. Sc, Y, La und Lanthanide, 8th Ed. (Springer, Berlin, 1976) pp. 50, 51, 98–100, 158, 159.
[2] A.V. Chadwick, D.S. Hope, G. Jaroszkiewicz and J.H. Strange, in: Fast ion transport in solids, eds. P. Vashishta, J.N. Mundy and G.K. Shenoy (North-Holland, Amsterdam, 1979) pp. 683–686.
[3] J. Schoonman, Solid State Ionics 1 (1980) 121.
[4] L.E. Nagel and M.O'Keeffe, in: Fast ion transport in solids, ed. W. van Gool (North-Holland, Amsterdam, 1973) pp. 165–172.
[5] R.W. Bonne and J. Schoonman, J. Electroanal. Chem. 89 (1978) 289, 301.
[6] A. Sher, R. Solomon, K. Lee and M.W. Muller, Phys. Rev. 144 (1966) 593.
[7] K. Lee and A. Sher, Phys. Rev. Letters 14 (1965) 1027.
[8] I.D. Raistrick, Ch. Ho, Y.W. Hu and R.A. Huggins, J. Electroanal. Chem. 77 (1977) 319.
[9] A.K. Jonscher, Nature 250 (1974) 191; 253 (1975) 717; J. Mater. Sci. 12 (1978) 553.
[10] R.D. Armstrong, T. Dickinson and P.M. Willis, J. Electroanal. Chem. 53 (1974) 389.
[11] R.D. Armstrong and R.A. Burnham, J. Electroanal. Chem. 72 (1976) 257.
[12] J. Schoonman and R.A. Huggins, J. Solid State Chem. 16 (1976) 413.
[13] M. Goldman and L. Shen, Phys. Rev. 144 (1966) 321.
[14] K.E.D. Wapenaar and J. Schoonman, J. Solid State Chem. 25 (1978) 31.
[15] Gmelin Handbuch der Anorganischen Chemie, Seltenerdelemente, Teil C3. Sc, Y, La und Lanthanide, 8th Ed. (Springer, Berlin, 1976) pp. 252–253.
[16] J. Schoonman, G.J. Dirksen and R.W. Bonne, Solid State Commun. 19 (1976) 783.
[17] T. Takahashi, H. Iwahara and T. Ishikawa, J. Electrochem. Soc. 124 (1977) 208.
[18] H. Schmalzried, Z. Physik. Chem. NF 105 (1977) 47.
[19] J.H. Kennedy and R.C. Miles, J. Electrochem. Soc. 123 (1976) 47.
[20] C. Lucat, G. Campet, J. Claverie, J. Portier, J.M. Réau and P. Hagenmuller, Mat. Res. Bull. 11 (1976) 167.
[21] C.O. Tiller, A.C. Lilly and B.C. LaRoy, Phys. Rev. B8 (1973) 4787.
[22] A. Kessler and J.E. Caffyn, J. Phys. C3 (1972) 1134.